Received: 30 June 2021 | Revised: 18 October 2021 | Accepted: 20 November 2021

DOI: 10.1002/jor.25226

RESEARCH ARTICLE

Journal of Orthopaedic Research®

A bovine nucleus pulposus explant culture model

Elias Salzer[1] | Vivian H. M. Mouser[1] | Marianna A. Tryfonidou[2] | Keita Ito[1]

[1]Orthopaedic Biomechanics, Department of Biomedical Engineering, Eindhoven University of Technology, Eindhoven, Noord-Brabant, The Netherlands

[2]Department of Clinical Sciences, Faculty of Veterinary Medicine, Utrecht University, Utrecht, The Netherlands

Correspondence
Keita Ito, Orthopaedic Biomechanics, Department of Biomedical Engineering, Eindhoven University of Technology, GEM-Z 4.115, PO Box 513, 5600 MB Eindhoven, The Netherlands.
Email: k.ito@tue.nl

Funding information
Horizon 2020 Research and Innovation Program, Grant/Award Number: #825925; Dutch Arthritis Society, Grant/Award Number: #LLP22

Abstract

Low back pain is a global health problem that is frequently caused by intervertebral disc degeneration (IVDD). Sulfated glycosaminoglycans (sGAGs) give the healthy nucleus pulposus (NP) a high fixed charge density (FCD), which creates an osmotic pressure that enables the disc to withstand high compressive forces. However, during IVDD sGAG reduction in the NP compromises biomechanical function. The aim of this study was to develop an ex vivo NP explant model with reduced sGAG content and subsequently investigate biomechanical restoration via injection of proteoglycan-containing notochordal cell-derived matrix (NCM). Bovine coccygeal NP explants were cultured in a bioreactor chamber and sGAG loss was induced by chondroitinase ABC (chABC) and cultured for up to 14 days. Afterwards, diurnal loading was studied, and explant restoration was investigated via injection of NCM. Explants were analyzed via histology, biochemistry, and biomechanical testing via stress relaxation tests and height measurements. ChABC injection induced dose-dependent sGAG reduction on Day 3, however, no dosing effects were detected after 7 and 14 days. Diurnal loading reduced sGAG loss after injection of chABC. NCM did not show an instant biomechanical (equilibrium pressure) or biochemical (FCD) restoration, as the injected fixed charges leached into the medium, however, NCM stimulated proliferation and increased Alcian blue staining intensity and matrix organization. NCM has biological repair potential and biomaterial/NCM combinations, which could better entrap NCM within the NP tissue, should be investigated in future studies. Concluding, chABC induced progressive, time-, dose- and loading-dependent sGAG reduction that led to a loss of biomechanical function.

Keywords
biomechanics | intervertebral disc | matrix degradation | low back pain | proteoglycans

1 | INTRODUCTION

Low back pain (LBP) is a worldwide physical and psychological health problem with growing socioeconomic burdens and prevalence.[1,2] The most common diagnosis for LBP is intervertebral disc degeneration (IVDD),[3] and the onset of human IVDD occurs earlier in life than in comparable tissues such as articular cartilage.[4]

IVDs are load-bearing cartilaginous joints between vertebral bodies that stabilize the spine while allowing movement. The IVD's central nucleus pulposus (NP), is covered superiorly and inferiorly by

cartilaginous endplates and is radially confined by the annulus fibrosus.[4] The healthy NP's extracellular matrix (ECM) consists primarily of proteoglycans, mainly aggrecans, and of randomly organized collagen fibers of mainly type II.[5,6] Aggrecan bears numerous sulfated glycosaminoglycans (sGAGs), for example, chondroitin sulfate (CS), which contain fixed negative charges. The resulting fixed charge density (FCD), a measure of fixed negative charges per volume, creates a high osmotic pressure that is important for biomechanical function of the IVD.[7] It is this mechanism—high water retention in the confined NP driven by osmotic pressure—which gives the IVD its outstanding biomechanical properties and the NP its importance to a healthy IVD. When external loads during axial compression are higher than the internal swelling stress (mainly osmotic pressure in the NP), water flows out and the height is reduced. Vice versa, the disc swells and increases in height when loads are lower than swelling stresses. When there is no net fluid loss or gain, the disc is at equilibrium and the swelling pressure is equal to the applied load.[8] Daily activity and night rest thereby lead to diurnal loading of the IVD in healthy as well as in degenerated conditions.

An early hallmark of IVDD is proteoglycan reduction in the NP[6] and thus a reduction of the FCD and swelling pressure.[9] This comes with drastic changes in mechanical behavior as the osmotic pressure[8] and hydration[6] reduces, while the NP-tissue flow permeability and solute diffusivity increase.[10] While severe symptomatic degenerated discs ultimately require surgery, the injection of cells, bioactive factors, and/or biomaterials forms a promising approach to functionally restore and regenerate mild to moderately degenerated discs. Previously, notochordal cell (NC)-derived NP matrix (NCM) has been suggested as an injectable biomaterial for IVD regeneration.[11,12] NCM is processed matrix, derived from the porcine NC-rich NP tissue, which is de-vitalized, lyophilized, pulverized, and rehydrated in saline for injection. NCM contains NC-derived factors, as well as a proteoglycan- and collagen-rich matrix that has the potential to biomechanically restore degenerated discs due to matrix replenishing capacity.

To this day, animal studies are indispensable for clinical translation, and safety and efficacy studies. However, their scientific impact is not commensurate with the substantial quantity of large animals used in IVD studies.[13] Ex vivo cultures enable studies in a controlled laboratory environment and have ethical advantages, while allowing higher throughput and flexibility.[14] Recently, NP explants gained attention as they allow a better control of sample geometries, degeneration state, and loading. Frequently, IVDD is enzymatically induced in ex vivo setups. Chondroitinase ABC (chABC) catalyzes the degradation of CS to mainly disaccharides and oligosaccharides. The activity and stability are strongly dependent on environmental conditions and were reported to be between 0.5 h and 10 days.[15–17]

The aim of this study was to (1) develop and analyze a bovine NP culture model and reduce the sGAG content via injection of chABC, (2) study the effect of diurnal loading on this model, and (3) elucidate whether NCM injection restores the biomechanical properties (tissue pressure) by increasing the FCD and thereby the swelling pressure to prevent progression of degenerative changes.

2 | MATERIALS AND METHODS

The experimental design is illustrated in Figure 1. If not stated otherwise, chemicals were purchased from Sigma-Aldrich.

2.1 | Nucleus pulposus explant culture

Bovine tails from 18 to 36 months old cows were purchased from a slaughterhouse in accordance with local regulations. Tissue explants were aseptically prepared within 24 h after the animal's death from the first 4–5 intact proximal discs. NP explants with 4–6 mm height and 8 mm diameter (200–300 mg) were harvested. The explants were

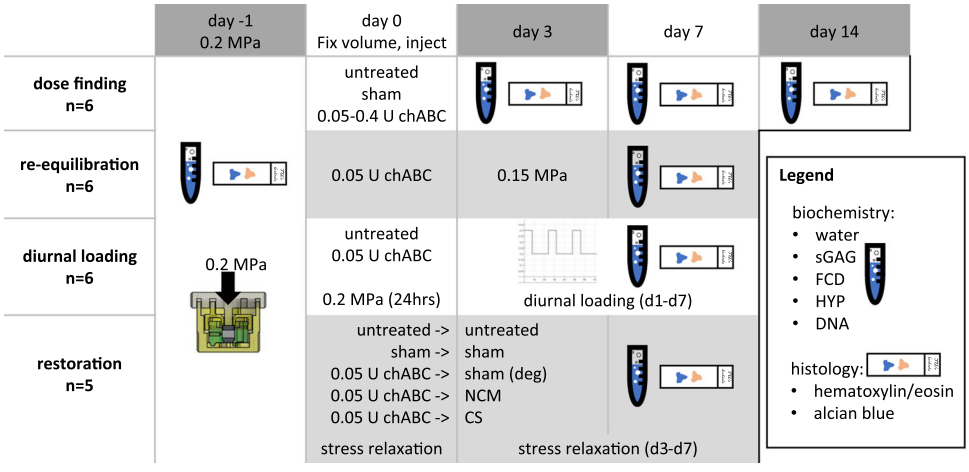

FIGURE 1 Experimental design to study degenerative changes after chABC injection ex vivo. Bovine nucleus pulposus samples were cultured in a bioreactor chamber and separated into several groups (dose-finding, re-equilibration, diurnal loading, and restoration). chABC, chondroitinase ABC; CS, chondroitin sulfate; FCD, fixed charge density; HYP, hydroxyproline; NCM, notochordal cell-derived matrix; sGAG, sulfated glycosaminoglycan; deg, degenerated

cultured under physiological conditions at 37°C, 5% O_2, and 10% CO_2 (i.e., pH = 7.2) to mimic the environment of nucleopulpocytes in vivo.[18] Medium consisted of low glucose (1 g/L) DMEM (21885, Gibco) with 1 mM sodium pyruvate, 3% fetal bovine serum (Greiner Bio-One), and 1% penicillin/streptomycin and was exchanged every 2–3 days. Medium osmolarity (346 mOsmol/L) was not artificially increased as NPs were cultured in confinement. To prevent swelling after the NP is released from its confined space between the vertebrae and encircled by the AF, we developed an NP bioreactor chamber based on a previous study.[19] This bioreactor chamber allows axial loading, mechanical testing, and contains a port for central injection (Figure 2). The NP tissue volume can be locked to an equilibrated internal pressure.

2.2 | Chondroitinase ABC dose evaluation

Freshly harvested NP tissue (Day - 1) served as native tissue controls ($n = 6$). All other explants were equilibrated to the same pressure of 0.2 MPa by adding weight for 16 h ($n = 6$/group/time point) and subsequently locking the volume with the locking lid and then cultured with a constant volume without added weight. This pressure was based on initial pressure of the tissue at harvest.[20] Consolidation for 16 h was found sufficient to reach equilibrium in preliminary experiments. Thereafter, tissue volume was locked, and height was measured with a benchtop thickness gauge (Checkline Europe). Untreated samples were cultured for 14 days to investigate matrix homeostasis. To reduce sGAGs, chondroitinase ABC (chABC, from *Proteus vulgaris* 50-250 units/mg, C3667, Sigma-Aldrich) was reconstituted in 1% bovine serum albumin (BSA) in phosphate-buffered saline (PBS) and stored at −20°C. Various doses of the enzyme (0.05, 0.1, 0.2, and 0.4 U) were injected centrally in the NP using a gastight 100 µl Hamilton syringe with a 27G needle (1710 RN) in a total volume of 20 µl. The effects of injection alone were controlled by a sham injection of 20 µl carrier (1% BSA in PBS). After the dose for inducing mild sGAG reduction was found, further studies were conducted using this dose (0.05 U/explant).

2.3 | Effect of loading on enzyme-treated explants

Bovine NP samples were equilibrated to 0.2 MPa as described above ($n = 6$ per group). Three days after inducing mild sGAG loss with 0.05 U chABC, tissue was re-equilibrated (re-equil.) to 0.15 MPa to study potential sGAG fragment leaching resulting from enzymatically induced matrix loss. Afterwards, the effect of low diurnal loading on enzyme-treated explants was studied and compared to untreated diurnally loaded tissue. Samples ($n = 6$ per group) were equilibrated to 0.2 MPa and injected with 0.05 U chABC (0.05 U diurnal) or no treatment (untreated diurnal). Following, samples were re-equilibrated for 24 h at 0.2 MPa to investigate immediate height loss, and subsequently, the explants were loaded diurnally for 7 days. Loading consisted of 8 h at 0.4 MPa followed by 16 h without load where the samples could swell back to the initially locked volume (after equilibration to 0.2 MPa). Tissue height was measured daily after samples creeped to 0.4 MPa.

2.4 | Partial biomechanical restoration via injection of NCM

Porcine NP was harvested from <12-week-old pigs that were obtained from a slaughterhouse according to local regulations. To obtain

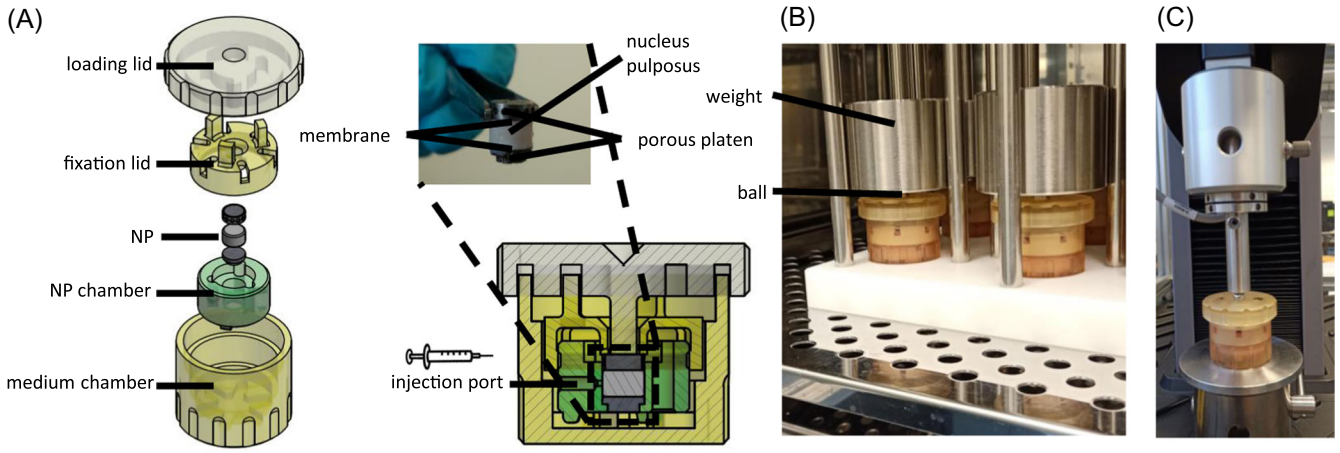

FIGURE 2 A bovine nucleus pulposus (NP) explant bioreactor chamber. (A) The NP is sandwiched between cellulose membranes (0.2 µm pore size) and 3 mm high, 316 L sintered stainless steel porous platens (200 µm pore size) in the NP chamber (polyether ether ketone (PEEK)). The top platen is surrounded by a stainless steel ring that allows smooth movement in the NP chamber's cylinder. The NP chamber is closed with the locking lid (PEEK) and placed in the medium chamber (polysulfone) which contains 4 ml medium. Pressure can be applied by placing a load on the loading lid (polysulfone), which is transmitted directly to the NP. (B) The NP tissue volume can be locked physically (fixation lid) to an equilibrated pressure to prevent tissue swelling. Biomaterials and fluids containing cells or growth factors can be injected via the injection port. (C) Tissue can be measured biomechanically with a tensile tester. Technical drawings were provided by Jurgen Bulsink

notochordal cell-derived matrix (NCM), the tissue was frozen at −80°C, lyophilized for 72 h (Freezone 2.4), pulverized, and reconstituted in a concentration of 300 mg/ml in PBS (30%). Devitalized NCM powder is rich in proteoglycans (Figure S2) and contains 632 ± 96 µg/mg sGAGs and 0.08 ± 0.04% residual DNA/dry weight. The reconstituted solution was further homogenized by injecting through a 27G needle. The NCM dose was based on partial restoration of sGAG content compared to a healthy level. To directly compare the restorative properties of injected sGAGs, Chondroitin sulfate C (chondroitin-6-sulfate, CS) from bovine trachea (27042, Sigma-Aldrich) was prepared in a concentration of 190 mg/ml in PBS, that is, a sGAG concentration similar to the sGAGs of the equivocal NCM dose which contains around 60% sGAGs whereas CS contains 100% sGAGs.

After equilibration to 0.2 MPa, five groups ($n = 5$ per group) were compared; an "untreated" group which did not receive any further treatment, a "sham"-injection group, where 20 and 25 µl PBS were slowly injected on Day 0 and Day 3, respectively. Mild sGAG loss was induced in the remaining three groups after equilibration to 0.2 MPa by injecting 0.05 U chABC at Day 0. After 72 h (on Day 3), either 25 µl PBS ("deg"), 19% CS ("CS"), or 30% NCM were injected ("NCM") through a 27G needle.

2.5 | Biomechanical testing

Biomechanical stress relaxation tests were performed at room temperature in the bioreactor chambers using a tensile tester (Figure 2C; MTS Criterion Model 42, MTS Systems Corporation). Pilot tests were performed to define measurement criteria. Samples were preconditioned by 3 initial ramps of 2% compression. Afterwards, a preload of 0.98 N was applied followed by displacement of 10% compression with a strain rate of 0.5 mm/s (approximately 10%/s) and held for 30 min while measuring force. Samples were tested directly after equilibration to 0.2 MPa (Day 0), before the second injection (Day 3), and, 24 h after the second injection, daily from Days 4 to 7. Data were analyzed using a custom written Matlab code (version R2018B, MathWorks). Peak and equilibrium stress were determined from experimental data. The time constant τ, which is a measure of tissue relaxation over time (t), was determined by fitting an exponential decay function to the relaxation of the stress relaxation curve (Equation 1), where σ is stress.

$$\sigma = \sigma_0 + \sigma_1 * e^{-\frac{t}{\tau}} \quad (1)$$

2.6 | Sample harvest

After culture, explants were harvested and cut into two parts for histology and biochemical analysis. For histology, samples were covered in Tissue-Tek (Sakura), frozen on dry ice, and stored at −20°C. Samples for biochemical analysis were weighed and stored at −80°C. Medium supernatant samples from diurnal loading and restoration experiments were taken on Days 0, 3, 5, and 7 and stored at −20°C.

2.7 | Biochemical assays

Frozen samples with known wet weight were lyophilized for 72 h after which dry weight was determined and relative water content was calculated. Thereafter, lyophilized samples were digested for 16 h at 60°C in 500 µl digestion buffer (100 mM phosphate buffer, 5 mM L-cystein, 5 mM EDTA) containing 1.8 U/ml papain from papaya latex (P-5306, Sigma-Aldrich).[21] DNA content was measured with the Qubit Fluorometric Quantitation method (Thermo Fisher Scientific) according to the user manual. Hydroxyproline (HYP) was measured with a chloramine-T assay[22] using trans-4-hydroxyproline (H5534, Sigma-Aldrich) as standard, reading absorbance at 550 nm. Sulfated GAG (sGAG) content was quantified by 1,9-dimethylmethylene blue (DMMB) binding assay at pH 3 using CS from shark cartilage (C4348, Sigma-Aldrich) as standard and extracting measured absorbance at 595 nm from 540 nm.[23] sGAG, DNA, and HYP content were normalized by dry weight. The FCD, in mEq/kg wet tissue, was estimated from the measured sGAG content (g), assuming a molecular weight of 502.5 g/mole for CS and a quantity of charge of 2 moles of charge per mole of sGAG.[24] FCD and sGAG values were compared to percent loss determined in macroscopically graded human degenerated discs reported by Antoniou et al. to determine the equivalent severity of degeneration according to sGAG loss (Table S1).[6,25,26] When medium was assessed to measure sGAG leaching, supernatant samples and standards were digested overnight in 50% v/v digestion buffer containing papain at 60°C as described above. The sGAG content was determined with a DMMB binding assay with standards diluted in full culture medium (50% v/v). The DMMB binding assay requires the length of the glycosaminoglycan chain be over a tetrasaccharide.[27] This means that molecules as small as disaccharides resulting from chABC digestion are not detectable with this assay and thereby do not contribute to the estimated FCD and sGAGs that leached into medium.

2.8 | Histological analysis

Eight µm thick cryosections (CM1950, Leica Biosystems) were collected on positively charged adhesion slides (SuperFrost Plus™, Thermo Fisher Scientific) and stored at −20°C. Sections were allowed to reach room temperature and were subsequently incubated at 37°C for 30 min to increase adherence. After fixation in 3.7% formalin for 5 min, samples were hydrated in water for 5 min and either stained with Mayer's hematoxylin (8 min) and Eosin Y (1 min), that is, H&E staining, to evaluate cellular changes or Alcian blue (30 min) to investigate proteoglycan content. Lactate dehydrogenase staining was performed to visualize viable cells.[28] Sections were dehydrated with ethanol, covered with Entellan and a cover glass for storage, and analyzed with a bright-field microscope (Axio Observer Z1, Zeiss).

2.9 | Statistical analysis

Statistical analysis was performed with R 4.0.2 and Graph Pad Prism 9.1.0. Normal distribution and equality of variances were

tested graphically by a quantile comparison plot followed by Levene's and Shapiro–Wilks' tests. Results are presented as mean ± one standard deviation. Statistical significance was assumed for $p < 0.05$.

One-way analysis of variance (ANOVA) (treatment) or two-way ANOVA (time-point and treatment) with post hoc Tukey's multiple comparison test was used to test for significance within groups or across multiple time points. When data were nonparametric, Kruskal–Wallis test with Dunn's multiple comparison test was performed. When data came from repeated measures, repeated measures two-way ANOVA with Tukey's multiple comparison test was performed. To determine the correlation of sGAG reduction and biomechanical behavior, a linear regression was fitted, and correlation was tested with nonparametric Spearman correlation tests.

3 | RESULTS

3.1 | Enzymatically induced sGAG reduction is dependent on dose, time, and loading

Healthy NP samples were injected with different doses of chABC and cultured for up to 14 days (Figure 3). On Day 3 after injection, a dose-dependent reduction of sGAG ranging to that expected in human IVDs with Thompson Grade 3 to 4[6,25,26] (Table S1) was observed (Figure 3A). On Day 3, the highest dose of chABC (0.4 U) significantly reduced sGAGs (18.8 ± 3.8% sGAGs/dw, $p = 0.0165$) compared to lowest concentration of chABC (0.05 U; 33.5 ± 9.7% sGAGs/dw), while there was no difference between 0.05 U chABC and sham injection (42.2 ± 6.6% sGAGs/dw). These dose-dependent effects faded and after 7 days there were no observable differences anymore between the chABC

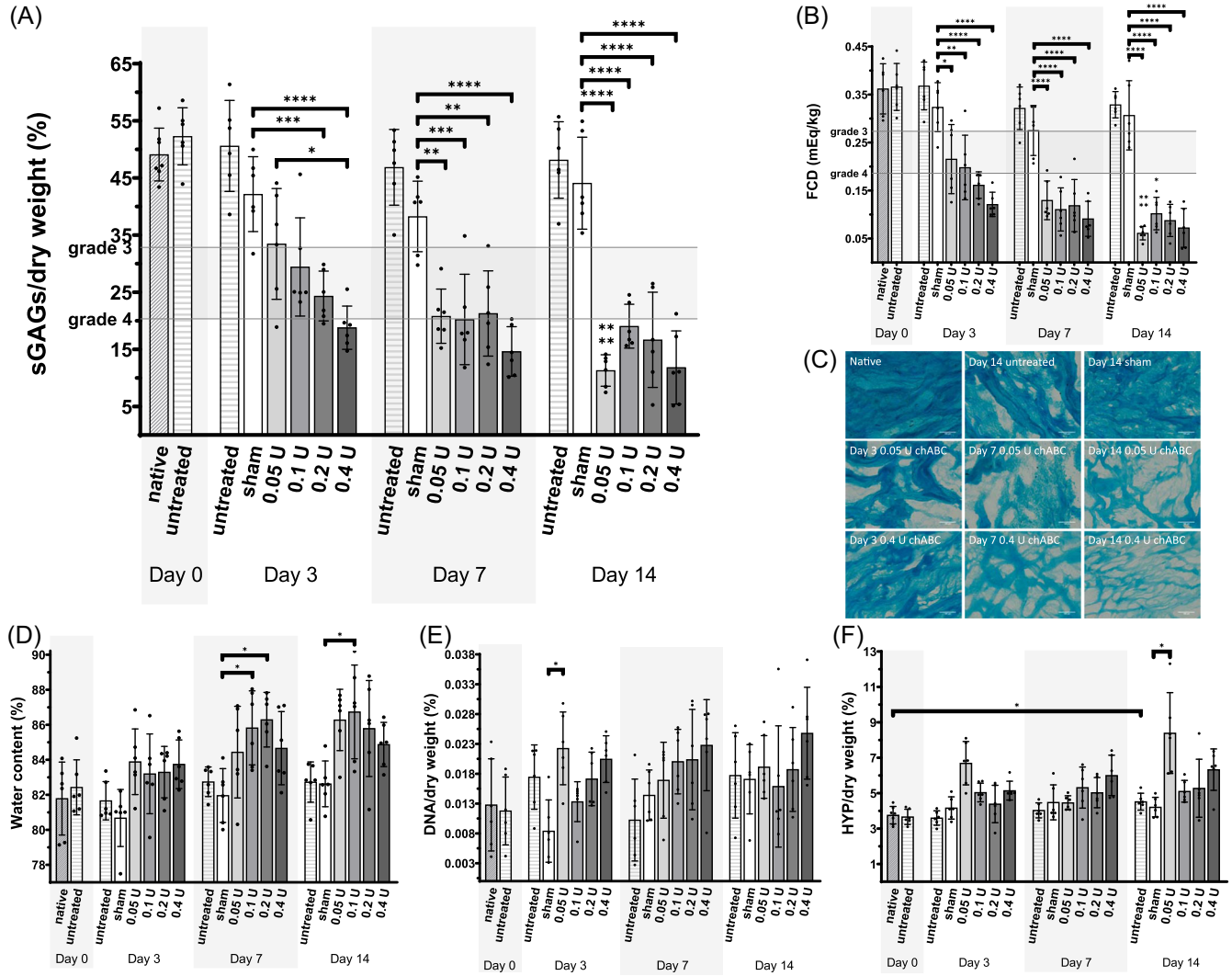

FIGURE 3 Sulfated glycosaminoglycan (sGAG) loss induced by injection of different doses of chondroitinase ABC (chABC). (A, B) The sGAG content and fixed charge density (FCD) are reduced in a dose- and time-dependent manner. (C) ChABC treated samples show matrix disorganization and reduced staining intensity (proteoglycan content) in Alcian blue stained sections. (D–F) Water content, DNA, and hydroxyproline (HYP) content remain mainly unchanged. For sGAGs and FCD reduction in grades 3 and 4 (gray lines) from human degeneration data are indicated. Scale bars: 100 µm. * $p < 0.05$; ** $p < 0.01$; *** $p < 0.001$; **** $p < 0.0001$. $n = 6$/group/time point

groups. Nonetheless, after 7 days all chABC groups contained significantly less sGAGs compared to the sham injection group. The FCD was decreased significantly after 3 days of culture when injecting 0.05 U chABC (0.22 ± 0.07 mEq/kg) compared to sham injection (0.32 ± 0.05 mEq/kg, Figure 3B). Alcian blue stained sections indicated the reduction of proteoglycan content and disorganization after injection of chABC compared to native, sham, and untreated samples (Figure 3C). Except for HYP content after 14 days (+0.8%), there were

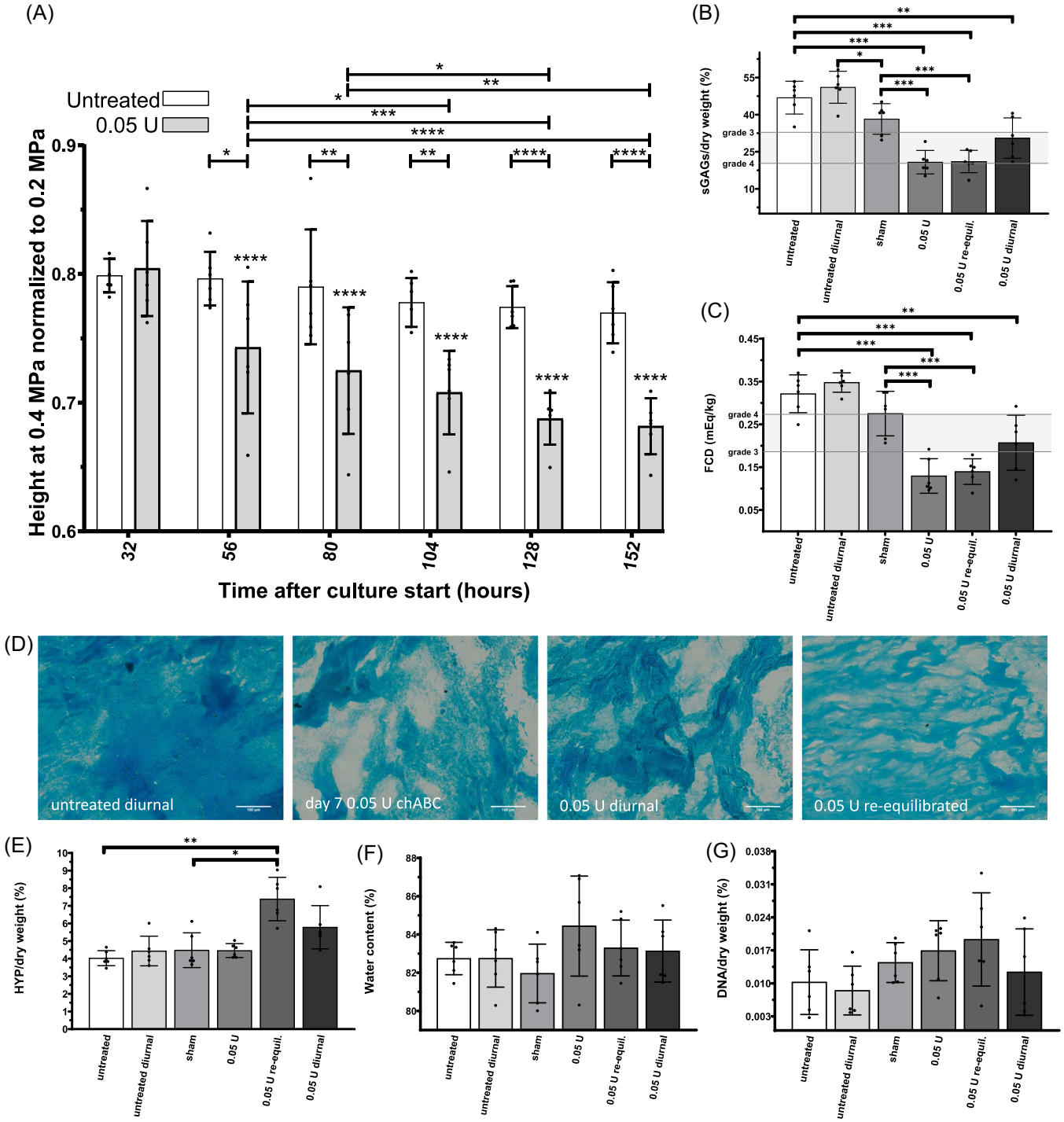

FIGURE 4 Loading influences enzyme kinetics. (A) Diurnally loaded samples creep more when they are treated with chABC. (B, C) Re-equilibration (Re-equil.) does not influence chondroitinase ABC (chABC) induced sGAG loss, but diurnal loading influences sulfated glycosaminoglycan (sGAG) content and FCD. (D) Alcian blue stained sections indicate proteoglycan loss in chABC treated groups. (E–G) Hydroxyproline, water, and DNA content remain mainly stable. Note that the Alcian blue stained Day 7 0.05 U chABC image is from the dose-finding experiment. Stars above bars in panel (A) indicate difference to 32 h measurements. *$p < 0.05$; **$p < 0.01$; ***$p < 0.001$; ****$p < 0.0001$. $n = 6$/group

no statistically significant biochemical differences between native samples and untreated samples, which indicates a stable culture system when no interventions are taken. While water content tended to increase in the enzyme injected samples (Figure 3D), DNA and HYP content were stable during culture (Figure 3E,F).

The effect of diurnal loading and re-equilibration was tested after injection of 0.05 U chABC. Untreated diurnally loaded samples were comparable to untreated samples in terms of biochemical outcomes (sGAGs, HYP, DNA, H_2O, and FCD; Figure 4). Re-equilibration after 3 days of enzyme injection to 0.15 MPa led to a mean height loss of 25% (data not shown). The equilibrium height of diurnally loaded samples (untreated or 0.05 U) was measured after equilibrating to 0.4 MPa and normalized to 0.2 MPa at Day 1 to obtain height loss in percent (-Figure 4A). When the load was increased in diurnally loaded explants from 0.2 to 0.4 MPa, height decreased in all groups. At 0.4 MPa, height was significantly reduced in 0.05 U treated compared to untreated diurnally loaded samples (around −30% and −20% on Day 7, respectively). Furthermore, height loss progressed over time in the 0.05 U chABC treated group whereas there were no significant differences within the untreated diurnally loaded group over the culture period. sGAG content (Figure 4B) and FCD (Figure 4C) of the 0.05 U (20.8 ± 4.75% sGAGs/dw) and re-equilibrated group (21.1 ± 4.5% sGAGs/dw) were significantly reduced compared to the untreated (46.9 ± 6.6% sGAGs/dw) and sham injected group (38.3 ± 6.2% sGAGs/dw). The 0.05 U diurnal group was significantly reduced in both, FCD and sGAG, only to the untreated diurnal but not sham injected group. In Alcian blue stained sections (-Figure 4D), less staining intensity was observed in the enzyme-treated groups compared to untreated diurnally loaded samples. The proteoglycan structure of the re-equilibrated sample appeared to be compressed compared to an isotropic appearance of the other groups. The HYP content (Figure 4E) was higher in re-equilibrated samples compared to the sham treatment. No differences between the groups were observed in the water (Figure 4F) and DNA content (Figure 4G).

sGAGs measured in the supernatants did not differ between the enzyme-treated and the untreated diurnally loaded samples (data not shown).

3.2 | NCM injection does not restore the NP due to sGAG diffusion

The ability of NCM to restore the NP tissue upon injection at biochemical and biomechanical levels was tested in enzyme-treated samples and compared to the effects of CS. The sGAG content (Figure 5A) between the 0.05 U (16.2 ± 5.9% sGAGs/dw), CS (19.6 ± 3.5% sGAGs/dw), and NCM (16.6 ± 2.8% sGAGs/dw) were not different, but all had significantly lower sGAG content than the two control groups (sham (37.6 ± 4.0% sGAGs/dw) and untreated (35.9 ± 1.6% sGAGs/dw)) and the native NP samples (39.9 ± 3.6% sGAGs/dw). The sGAGs released from the NP tissue were measured in the medium supernatant over time (Figure 5B). On Day 5, 48 h after injection of CS or NCM, there was an increased release of sGAGs in both groups compared to sham treatment and the 0.05 U injected group. Note that medium was exchanged on Days 3 and 5. Alcian blue stained sections showed disorganized ECM due to chABC injection (Figure 5C). Even though the staining intensity was reduced in the NCM group compared to native explants, the matrix appeared less disorganized and slightly increased compared to chABC- and CS-treated explants. The DNA content (Figure 5D) of the NCM injected group was significantly increased compared to all other groups; mean DNA content was above the indicated "expected value" from residual DNA of the injected NCM. On H&E stained sections, two very distinct regions of the NP tissue were observed only in the NCM group: unorganized matrix with nuclear fragmented pieces and organized tissue with clear cellular structures and indications of cell clustering (Figure 5E). The water content of the enzyme-treated groups (0.05 U (84.9 ± 0.9%), CS (84.6 ± 1.1%), and NCM (84.1 ± 1.2%)) was significantly increased compared to the native samples (80.3 ± 1.9%; Figure 5F). There was no difference in HYP content between groups (Figure 5G). The FCD (Figure 5H) followed the sGAG results.

When assessing biomechanical properties in stress relaxation, a typical stress relaxation curve was obtained with an initial peak pressure followed by decrease of stress over time. The equilibrium pressure revealed that the adjusted pressure of 0.2 MPa (0.23 ± 0.03 MPa) was reached after overnight equilibration on Day 0 (Figure 6A; day 0). After injection of chABC on Day 0, the NP tissue was cultured for 72 h, which lead to a loss of around 50% of equilibrium pressure on Day 3 (0.08 ± 0.03 MPa) (Figure 6A). Subsequent injection of CS or NCM did not restore the equilibrium stress. The peak stress showed large variances and compared to Day 0 it increased in the sham and untreated group (Figure S1). Tissue relaxation, τ, followed the results observed for the equilibrium stress (Figure 6B). Starting on Day 4, there was a significant reduction compared to sham injection. There were strong positive correlations between FCD and equilibrium stress and relaxation time constant, τ, (Figure 6C), illustrating that explants with a higher FCD also have a higher equilibrium stress (intradiscal pressure) and a longer tissue relaxation time (slower pressure loss). Peak stress showed no correlations to equilibrium stress, τ or FCD (Figure S1).

3.3 | Cells remain viable in various culture conditions in NP explant bioreactor chambers

Cells remained viable in all tested conditions visualized by LDH staining and NCM injected samples had additionally large clusters of living cells (Figure 7).

4 | DISCUSSION

In this study, we present an ex vivo cultured bovine coccygeal NP explant model where progressive sGAG loss was induced via injecting of chABC. The severity of the enzymatic activity was dose-, time-, and loading-dependent and a decrease in osmotic pressure was not restored via injection of NCM or CS, as fixed charges leached into the medium.

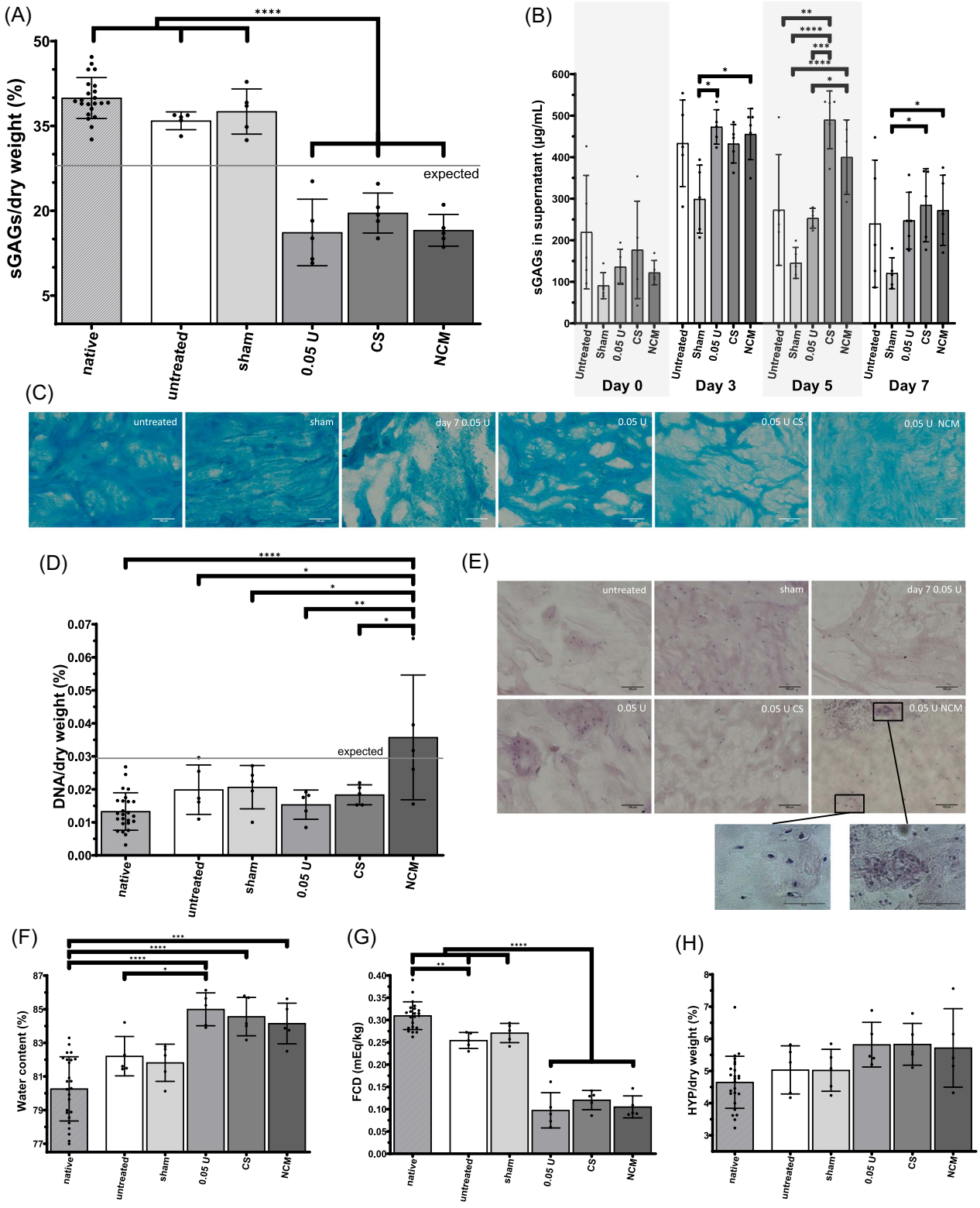

FIGURE 5 Biochemical differences and histology after injection of notochordal cell-derived matrix (NCM) or chondroitin sulfate (CS). (A) Glycosaminoglycan (sGAG) content is different from controls, but not within the chABC treated groups. (B) On Day 5, part of the injected sGAG (NCM and CS group) leaches into the medium. (C) The Alcian blue staining intensity is decreased in chABC treated groups. (D) DNA is increased in NCM injected groups. (E) Hematoxylin & eosin stained sections indicate that there are tissue regions with different characteristics containing either remnant of NCM recognized by residual DNA (dark and condensed dots) in the tissue or cell clusters of living cells identified by a translucent cell shape around a cell nuclear core. (F) Water content is increased and (G) FCD decreased in the chABC treated groups compared to the control groups. (H) The hydroxyproline content does not change. The expected sGAG and DNA content from NCM injections are indicated in the sGAG and DNA figure, respectively. Scale bars: 100 µm (overview) and 50 µm (close-ups of NCM). *$p < 0.05$; **$p < 0.01$; ***$p < 0.001$; ****$p < 0.0001$. $n = 5$/group

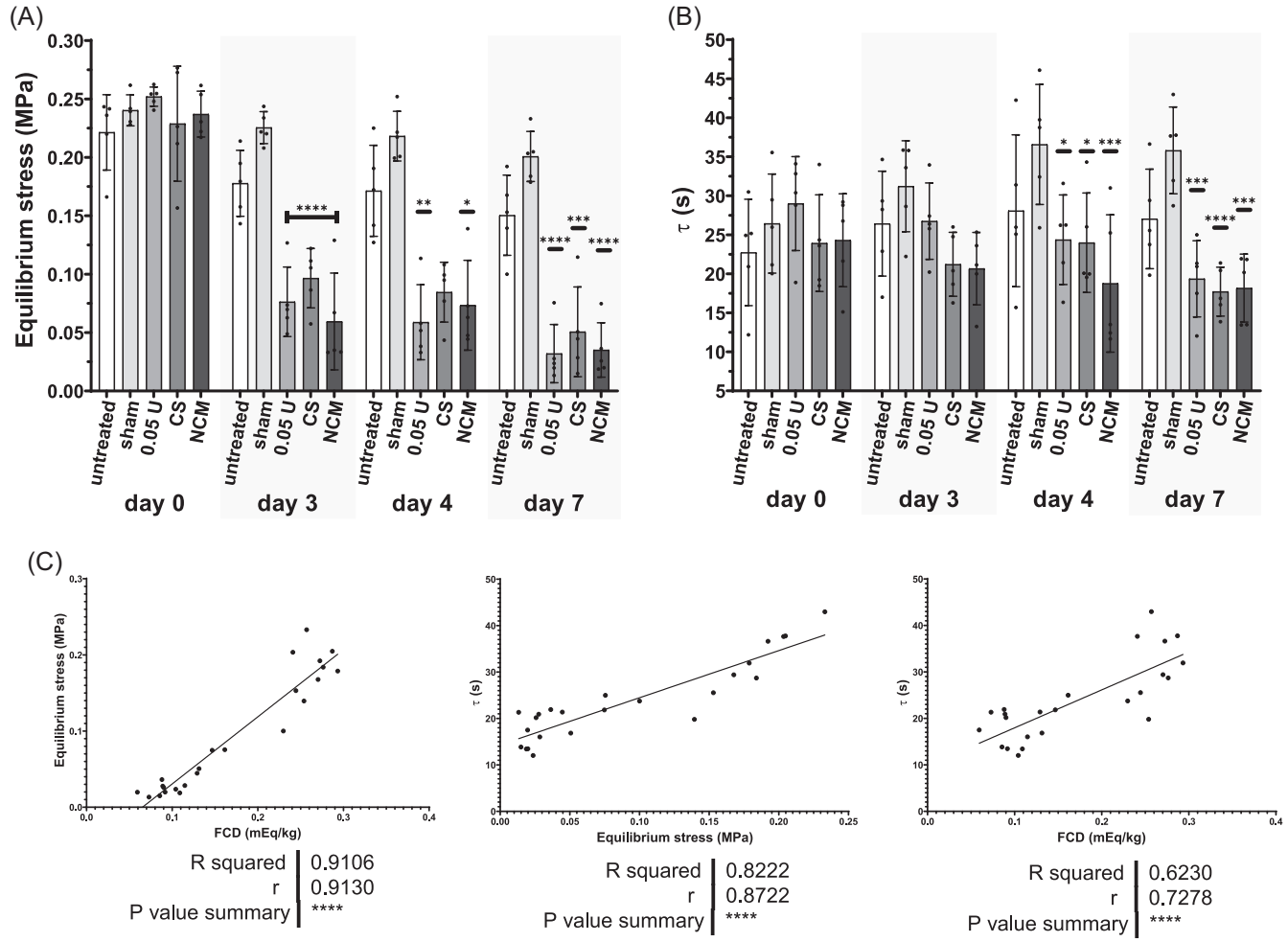

FIGURE 6 Biomechanical evaluation of chACB treated nucleus pulposus and correlation to fixed charge density (FCD). (A) Equilibrium stress is around 0.2 MPa on Day 0, but drops after injection of chondroitinase ABC (Day 3) and is not restored after injecting notochordal cell-derived matrix (NCM) or chondroitin sulfate (CS) (Days 4 and 7). (B) The tissue relaxation, τ, follows the same trend as the equilibrium pressure. Stars indicate significance compared to Day 0 for equilibrium stress or compared to sham of the same day for τ. (C) FCD, equilibrium stress, and τ are all positively correlated. For equilibrium stress, Day 0 (all untreated) as well as the three sGAG treated groups on Day 3 were summarized for statistical testing. Correlations of biomechanical data received from stress relaxation testing and FCD are from Day 7. $^{*}p < 0.05$; $^{**}p < 0.01$; $^{***}p < 0.001$; $^{****}p < 0.0001$. $n = 5$/group

4.1 | Enzymatically induced sGAG loss

The present study shows progressive sGAG loss after injection of chABC, which is in line with previous studies. Furthermore, the dose that we used (0.05–0.4 U or 0.2–1.6 U/NP) is comparable to that used in various other studies with different tissue volumes (summarized in Table 1). In a very similar experimental setup, Krupkova et al.[39] reported a less profound sGAG reduction compared to our system. As they used a dialysis membrane, larger functional proteoglycan fragments could potentially have been contained. Even though chABC is frequently used to induce sGAG loss, sGAG reduction, fragmentation, and aging are more complex during human IVDD. ChABC did not activate cellular responses in bovine NP tissue at 2 weeks follow-up,[39] however, inflammatory cytokines and catabolic enzymes were increasingly expressed in a goat model at 12 weeks follow-up.[31] Cellular reactions might be due to an osmotic shock or due to degrading products of CS resulting from chABC cleavage, as the latter were found to change morphology and induce catabolic expression in chondrocytes in 3D culture.[40] Furthermore, a distorted physical and biochemical microenvironment might be a trigger for resident cells to go into a "pro-inflammatory state."[41] In this study, cells remained viable in all tested conditions. Nevertheless, the long-term response of cells to chABC injection remains unclear.

4.2 | The relevance of loading

We demonstrate that explants equilibrated to 0.2 MPa, which corresponds to human discs at rest,[42] cultured at a constant volume, were able to maintain tissue matrix composition and properties comparable to native samples. Furthermore, diurnal loading changed the

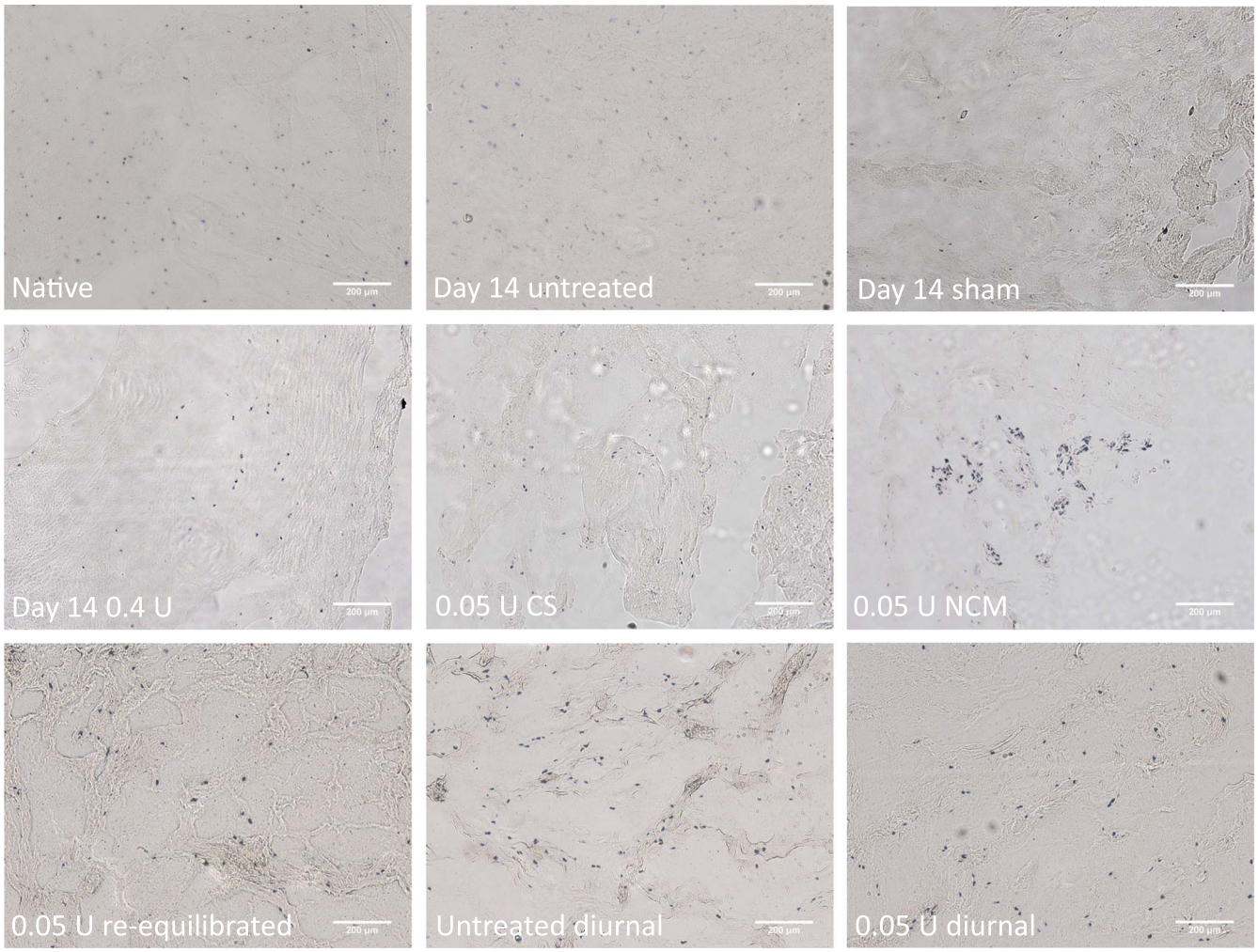

FIGURE 7 Evaluation of viable nucleus pulposus cells after culture in the bioreactor chamber with fixed volume. Lactate dehydrogenase staining revealed viable cells in all tested conditions. NCM injected samples had additionally large clusters of living cells. Scale bars: 200 µm. NCM, notochordal cell-derived matrix

enzyme kinetics of chABC and thereby reduced sGAG loss compared to unloaded samples. As transport of large proteins may be affected by diurnal convection but not by physiological dynamic loading (~0.1–10 Hz), this was the component studied. We hypothesize, that increased convection due to diurnal consolidation is the main driver of the effect observed (diluting the enzyme). Similar to our results, Gawri et al.[43] have reported restoration of sGAG content when comparing loaded and unloaded trypsin-treated bovine discs, which they attribute to new ECM production. To this respect, recapitulating some aspects of physiological conditions seems to be an essential factor when studying disc degeneration in ex vivo cultures.

Diurnal loading did not increase sGAG diffusion, as sGAGs in supernatant between enzyme-treated and untreated diurnally loaded samples were at similar levels. Therefore, we hypothesize that increased permeability due to reduced FCD does, in our system, not directly lead to diffusion of larger negatively charged molecules. This is further supported by findings that re-equilibrated tissue could not prevent sGAG loss from the tissue. For small molecules, it has been described that diffusion is the main mechanism of transport rather than convective transport.[44] Nevertheless, sGAG reduction was to a lesser extent when tissue was loaded diurnally. We believe that this is the result of changed enzymatic activity due to convective transport of the enzyme.

4.3 | ChABC induced sGAG loss leads to loss of biomechanical functionality

In this study, we show that chABC-induced sGAG loss directly impairs biomechanical function. In GAG-rich tissues, like the IVD and cartilage, sGAG content is directly related to FCD. FCD reduction decreases the swelling potential, which can be measured by the equilibrium stress in a stress relaxation test where at equilibrium, most of the load is carried by osmotic swelling pressure.[45] sGAG reduction induced by chABC had minimal effects on peak stress but reduced equilibrium stress, comparable to cartilage.[46]

During human IVDD, a catabolic shift leads to degradation and fragmentation of proteoglycans in the NP, which is hypothesized to

TABLE 1 Chondroitinase ABC (chABC) dose used in intervertebral disc degeneration studies compared to nucleus pulposus (NP) volume

Study	Model/NP volume/duration	chABC	Degeneration description
[29]	In vivo caprine lumbar IVD	0.2–0.35 U/ml (110–200 µl):	Slowly progressive degeneration
	740 µl[30]	0.022–0.07 U	
	26 weeks	0.03–0.1 U/NP	
[31,32]	In vivo caprine lumbar IVD	0.5–25 U/ml in 200 µl:	Progressive degeneration mild (0.1 U), moderate (1 U), severe (5 U)
	740 µl[30]	0.1–5 U	
	12 weeks	0.14–6.8 U/NP	
[33]	In vivo ovine lumbar IVD	5 U/ml in 200 µl	Progressive, severe degeneration
	656 µl[34]	1 U	
	17 weeks	1.52 U/NP	
[35]	In vivo ovine lumbar IVD	5–250 U/ml in 200 µl	Progressive, severe degeneration
	656 µl[34]	1, 5, 50 U	
	4 weeks	1.52–76.2 U/NP	
[36]	In vivo ovine lumbar IVD	1 U	Progressive degeneration
	656 µl[34]	1.52 U/NP	
	24 weeks		
[37]	Ex vivo loaded lumbar caprine IVD	0.5 U/ml (100 µl):	Progressive, mild degeneration
	620 µl (173 mm^2[2,30] and 3.6 mm height)	0.05 U	
	3 weeks	0.08 U/NP	
[38]	Ex vivo loaded lumbar caprine IVD	2 U/ml chABC + 1 mg/ml collagenase in 50 µl	Progressive, moderate degeneration
	740 µl[30]	0.1 U chABC	
	10 days	0.14 U/NP	
[39]	Ex vivo coccygeal bovine NP	1–20 U/ml in 20 µl:	Concentration-dependent sGAG reduction
	250 µl	0.02–0.4 U	
	3 weeks	0.08-1.6 U/NP	
This study	Ex vivo (loaded) coccygeal bovine NP	2.5–20 U/mL in 20 µL:	Time, concentration, and loading dependent mild to severe progressive degeneration
	250 µl	0.05-0.4 U	
	2 weeks	0.2-1.6 U/NP	

start a vicious cycle of IVDD.[47] As smaller proteoglycans leach out of the tissue and cells have an insufficient anabolic response, the sGAG concentration and FCD in the NP decrease with increasing degeneration (Table S1).[6] Similarly, tonicity-dependent sGAG leaching was reported in bovine NP explants, with the highest sGAG loss in free swelling explants.[48] Additionally, sGAG leaching was reported to be increased in loaded bovine disc cultures in degenerative medium compared to healthy medium.[49] Disc height loss, a hallmark of IVDD, was demonstrated in this study by increased height loss in enzyme-treated diurnally loaded explants. Other hallmarks of IVDD that concern the CEP and AF and their interplay with the NP cannot be mimicked in our NP model. Additionally, the human NP loses water during IVDD[6] whereas the water content tended to increase after chABC injection in our study, potentially as water replaces the lost matrix due to the fixed volume. Comparable to human IVDD, biomechanical changes occurred after chABC injection, as hydraulic pressure in the tissue decreased and the creep increased compared to untreated samples. The NP, when surrounded by the CEP and AF, is expected to be less permeable than our culture system, as even small molecules were illustrated to remain within the disc.[50] Cartilage's permeability and FCD correlate[10] and Alice Maroudas suggested that the side chains of proteoglycans, GAGs, provide most of cartilage's resistance to fluid flow.[51] Diffusivities of larger molecules have also been reported to be dependent on GAG content.[52] This is in line with our findings that biomechanical properties (equilibrium stress, τ) and biochemical composition (FCD) strongly correlate. Additionally, chABC lead to visible microscopic ECM disorganization demonstrated on Alcian blue stained sections of enzyme-treated

bovine NP tissue. We believe this to be a proteoglycan-covered collagen network, where hyaluronan molecules and GAGs close to the collagen fibrils remain intact.

We found an increased equilibrium creep of enzyme-treated compared to untreated NP explants when loaded for 8 h at 0.4 MPa, recapitulating pressure in human discs at low activity.[42] This reduced weight-bearing capacity would lead in vivo to decreased disc height, a hallmark of IVDD. Increased creep and height loss in chABC-injected discs were found in a sheep model.[33] Interestingly, Paul et al.[37] reported an immediate change (initial creep) in chABC-treated and sham-injected goat discs ex vivo. As such, it is more plausible that ECM damage occurred due to injection of a large volume (100 µl), as enzymatic degradation might not have an immediate effect. In a rat tail model, a critical injection volume was reported above which degenerative changes occurred.[53] Therefore, we advise that high fluid shear forces should be prevented by slow and careful injection of small volumes to not harm the NP and resident/injected cells. Additionally, AF damage can be avoided by using small gauge needles.[54]

4.4 | Biomechanical restoration and biological repair

In preliminary experiments utilizing the lumbar caprine goat in a loaded organ culture model, NCM delayed the progression of disc height loss directly after injection.[55] In this study, a single injection of NCM or CS could not restore the biomechanical compressive behavior in terms of equilibrium stress, used as an indication of intradiscal pressure. This was unexpected, as substantial amounts of fixed charges were injected (to restore 50% of the FCD) in both the NCM and CS groups. Upon NCM injection, tissue FCD did not become increased due to the immediate loss of the injected sGAGs into the medium. Thus, in systems where CEP and AF integrity are no longer sustained to act as barrier for molecular loss (e.g., post-hernia), any added molecules would need to be in a more complex molecular structure or incorporated into a biomaterial as carrier to integrate into the tissue and contribute to the swelling pressure. NCM has been shown to induce other metabolic beneficial effects in vitro as well as in vivo and to stimulate cell proliferation in 3D and organoid cultures.[11,12,56] This was consistent with the increased DNA content above that which originated from the injected NCM itself supporting that NCM might contain growth factors that stimulate proliferation. This was also consistent with the observation on H&E stained sections in NCM-treated explants where cells appeared in clusters (indication of cloning) which we interpret as proliferation. However, cell clustering is also described in physically disrupted discs and is thought to arise from disturbed cell–matrix binding.[41] Thus, although we could not observe a direct biomechanical augmentation due to leakage of injected sGAG, potential metabolic effects were evident. Additionally, NCM-injected explants showed a higher staining intensity and increased organization compared to sham and CS injected explants, which we believe to be larger molecules that were not lost (e.g., hyaluronan).

5 | CONCLUSION

We demonstrate the development of a platform to screen regenerative strategies of injectable biomaterials and cells for NP explants with sGAG reduction found in mildly degenerated human discs. To increase the clinical relevance of our platform, follow-up studies with human NP explants (e.g., at various degeneration states) with simulated physiological loading conditions may be investigated. To the best of our knowledge, this is the only NP culture system with a constant volume which is important for sustaining the natural environment of native cells. Tissue damage via a loss of ECM structure and sGAG content directly leads to compromised biomechanical function. Furthermore, by triggering sGAG loss, a cascade of degeneration inductive factors is started. Enzyme-treated NP tissue could not be restored by injecting NCM or CS due to sGAG leakage, but cellular proliferation and increased Alcian blue staining after NCM injection was observed.

The here presented culture system is a tool toward developing treatments for patients who suffer from mild to moderate disc degeneration. In future studies, the proliferative effect of NCM should be investigated as well as potential delivery of (decellularized) NCM together with a biomaterial to facilitate NCM retention and tissue integration.

ACKNOWLEDGMENTS

The authors would like to thank Jurgen Bulsink for technical drawings, designs, and manufacturing of the bioreactor chambers and deadweights. This project received funding from the European Union's Horizon 2020 Research and Innovation Program iPSpine under Grant agreement #825925 (www.ipspine.eu). MAT is supported by the Dutch Arthritis Society (#LLP22).

CONFLICT OF INTERESTS

ES and VHMM have no conflict of interest to declare. KI is a paid consultant and shareholder at NC Biomatrix, deputy editor of the Global Spine Journal and on the editorial board of Biomechanics and Modeling in Mechanobiology. MAT is on the scientific advisory board of JOR Spine and scientific advisor of SentryX.

AUTHOR CONTRIBUTIONS

All authors contributed to research design; Elias Salzer acquired and analyzed data; all authors interpreted data. Elias Salzer drafted the manuscript and all authors revised it critically. All authors have read and approved the final submitted manuscript.

ORCID

Elias Salzer http://orcid.org/0000-0001-8711-4243
Marianna A. Tryfonidou http://orcid.org/0000-0002-2333-7162
Keita Ito http://orcid.org/0000-0002-7372-4072

REFERENCES

1. Hartvigsen J, Hancock MJ, Kongsted A, et al. What low back pain is and why we need to pay attention. *Lancet*. 2018;391(10137):2356-2367.

2. Manchikanti L, Singh V, Falco FJE, Benyamin RM, Hirsch JA. Epidemiology of low back pain in adults. *Neuromodulation*. 2014;17(S2):3-10.
3. Ravindra VM, Senglaub SS, Rattani A, et al. Degenerative lumbar spine disease: estimating global incidence and worldwide volume. *Glob Spine J*. 2018;8(8):784-794.
4. Urban JPG, Roberts S. Degeneration of the intervertebral disc. *Arthritis Res Ther*. 2003;5(3):120-130.
5. Eyre DR, Muir H. Quantitative analysis of types I and II collagens in human intervertebral discs at various ages. *BBA - Protein Struct*. 1977;492(1):29-42.
6. Antoniou J, Steffen T, Nelson F, et al. The human lumbar intervertebral disc - Evidence for changes in the biosynthesis and denaturation of the extracellular matrix with growth, maturation, ageing, and degeneration. *J Clin Invest*. 1996;98(4):996-1003.
7. Roughley PJ, Mort JS. The role of aggrecan in normal and osteoarthritic cartilage. *J Exp Orthop*. 2014;1(1):1-11.
8. Urban JPG, McMullin JF. Swelling pressure of the lumbar intervertebral discs: Influence of age, spinal level, composition, and degeneration. *Spine*. 1988;13(2):179-181.
9. Perie DS, Maclean JJ, Owen JP, Iatridis JC. Correlating material properties with tissue composition in enzymatically digested bovine annulus fibrosus and nucleus pulposus tissue. *Ann Biomed Eng*. 2006;34(5):769-777.
10. Maroudas A. Physicochemical properties of cartilage in the light of ion exchange theory. *Biophys J*. 1968;8(5):575-595.
11. de Vries S, van Doeselaar M, Meij B, et al. Notochordal cell matrix as a therapeutic agent for intervertebral disc regeneration. *Tissue Eng Part A*. 2018:25(11-12):830-841.
12. Bach FC, Tellegen AR, Beukers M, et al. Biologic canine and human intervertebral disc repair by notochordal cell-derived matrix: from bench towards bedside. *Oncotarget*. 2018;9(41):26507-26526.
13. Reitmaier S, Graichen F, Shirazi-Adl A, Schmidt H. Separate the sheep from the goats: use and limitations of large animal models in intervertebral disc research. *J Bone Jt Surg Am*. 2017;99(19:e102):1-11.
14. Pfannkuche J-J, Guo W, Cui S, et al. Intervertebral disc organ culture for the investigation of disc pathology and regeneration – benefits, limitations, and future directions of bioreactors. *Connect Tissue Res*. 2020:61(3-4):304-321.
15. Ernst S, Langer R, Cooney CL, Sasisekharan R. Enzymatic degradation of glycosamnoglycans. *Crit Rev Biochem Mol Biol*. 1995;30(5):387-444.
16. Tester NJ, Plaas AH, Howland DR. Effect of body temperature on chondroitinase ABC's ability to cleave chondroitin sulfate glycosaminoglycans. *J Neurosci Res*. 2007;85:1110-1118.
17. Lin R, Kwok JCF, Crespo D, Fawcett JW. Chondroitinase ABC has a long-lasting effect on chondroitin sulphate glycosaminoglycan content in the injured rat brain. *J Neurochem*. 2008;104:400-408.
18. Urban JPG. The role of the physicochemical environment in determining disc cell behaviour. *Biochem Soc Trans*. 2002;30(6):858-864.
19. Arkesteijn IT, Mouser VH, Mwale F, van Dijk BG, Ito K. A well-controlled nucleus pulposus tissue culture system with injection port for evaluating regenerative therapies. *Ann Biomed Eng*. 2015;44(5):1798-1807.
20. Oshima H, Ishihara H, Urban JPG, Tsuji H. The use of coccygeal discs to study intervertebral disc metabolism. *J Orthop Res*. 1993;11(3):332-338.
21. Kim YJ, Sah RLY, Doong JYH, Grodzinsky AJ. Fluorometric assay of DNA in cartilage explants using Hoechst 33258. *Anal Biochem*. 1988;174(1):168-176.
22. Huszar G, Maiocco J, Naftolin F. Monitoring of collagen and collagen fragments in chromatography of protein mixtures. *Anal Biochem*. 1980;105(1):424-429.
23. Farnadale RW, Sayers CA, Barrett AJ. A direct spectrophotometric microassay for sulphated glycosaminoglycans in cartilage cultures. *Connect Tissue Res*. 1982;9(4):247-248.
24. Urban JPG, Maroudas A. The measurement of fixed charged density in the intervertebral disc. *BBA - Gen Subj*. 1979;586(1):166-178.
25. Antoniou J, Pike GB, Steffen T, et al. Quantitative magnetic resonance imaging in the assessment of degenerative disc disease. *Magn Reson Med*. 1998;40(6):900-907.
26. Antoniou J, Demers CN, Beaudoin G, et al. Apparent diffusion coefficient of intervertebral discs related to matrix composition and integrity. *Magn Reson Imaging*. 2004;22(7):963-972.
27. Coulson-Thomas VJ, Gesteira TF. Dimethylmethylene blue assay (DMMB). *Bio-protocol*. 2014;4(18):1-4.
28. Stoddart MJ, Furlong PI, Simpson A, Davies CM, Richards RG. A comparison of non-radioactive methods for assessing viability in ex vivo cultured cancellous bone: technical note. *Eur Cells Mater*. 2006;12:16-25.
29. Hoogendoorn RJ, Wuisman PI, Smit TH, Everts VE, Helder MN. Experimental intervertebral disc degeneration induced by chondroitinase ABC in the goat. *Spine*. 2007;32(17):1816-1825.
30. Showalter BL, Beckstein JC, Martin JT, et al. Comparison of animal discs used in disc research to human lumbar disc: torsion mechanics and collagen content. *Spine*. 2012;37(15):1-17.
31. Zhang C, Gullbrand SE, Schaer TP, et al. Inflammatory cytokine and catabolic enzyme expression in a goat model of intervertebral disc degeneration. *J Orthop Res*. 2020;38(11):2521-2531.
32. Gullbrand SE, Malhotra NR, Schaer TP, et al. A large animal model that recapitulates the spectrum of human intervertebral disc degeneration. *Osteoarthr Cartil*. 2017;25(1):146-156.
33. Borem R, Walters J, Madeline A, et al. Characterization of chondroitinase-induced lumbar intervertebral disc degeneration in a sheep model intended for assessing biomaterials. *J Biomed Mater Res Part A*. 2021;109(7):1232-1246
34. Beckstein JC, Sen S, Schaer TP, Vresilovic EJ, Elliott DM. Comparison of animal discs used in disc research to human lumbar disc: axial compression mechanics and glycosaminoglycan content. *Spine*. 2008;33(6):E166-E173.
35. Sasaki M, Takahashi T, Miyahara K, Hirose T. Effects of chondroitinase ABC on intradiscal pressure in sheep: an in vivo study. *Spine*. 2001;26(5):463-468.
36. Ghosh P, Moore R, Vernon-Roberts B, et al. Immunoselected STRO-3+ mesenchymal precursor cells and restoration of the extracellular matrix of degenerate intervertebral discs. *J Neurosurg Spine*. 2012;16(5):479-488.
37. Paul CPL, Emanuel KS, Kingma I, et al. Changes in intervertebral disk mechanical behavior during early degeneration. *J Biomech Eng*. 2018;140(9).
38. Rustenburg C, Snuggs J, Emanuel K, et al. Modelling the catabolic environment of the moderately degenerated disc with a caprine ex vivo loaded disc culture system. *Eur Cells Mater*. 2020;40:21-37.
39. Krupkova O, Hlavna M, Amir Tahmasseb J, et al. An inflammatory nucleus pulposus tissue culture model to test molecular regenerative therapies: validation with epigallocatechin 3-gallate. *Int J Mol Sci*. 2016;17(10):1-18.
40. Jung YK, Park HR, Cho HJ, et al. Degrading products of chondroitin sulfate can induce hypertrophy-like changes and MMP-13/ADAMTS5 production in chondrocytes. *Sci Rep*. 2019;9(15846):1-11.
41. Lama P, Claireaux H, Flower L, et al. Physical disruption of intervertebral disc promotes cell clustering and a degenerative phenotype. *Cell Death Discov*. 2019;5(154):1-9.
42. Wilke H-J, Neef P, Caimi M, Hoogland T, Claes LE. New in vivo measurements of pressures in the intervertebral disc in daily life. *Spine*. 1999;24(8):755-762.
43. Gawri R, Moir J, Ouellet J, et al. Physiological loading can restore the proteoglycan content in a model of early IVD degeneration. *PLOS One*. 2014;9(7):1-8.
44. Urban JPG, Smith S, Fairbank JCT. Nutrition of the intervertebral disc. *Spine*. 2004;29(23):2700-2709.

45. Quiroga JMP, Wilson W, Ito K, van Donkelaar CC. Relative contribution of articular cartilage's constitutive components to load support depending on strain rate. *Biomech Model Mechanobiol*. 2017;16(1):151-158.
46. Korhonen RK, Laasanen MS, Töyräs J, Lappalainen R, Helminen HJ, Jurvelin JS. Fibril reinforced poroelastic model predicts specifically mechanical behavior of normal, proteoglycan depleted and collagen degraded articular cartilage. *J Biomech*. 2003;36(9):1373-1379.
47. Buckwalter JA. Aging and degeneration of the human intervertebral disc. *Spine*. 1995;20(11):1307-1314.
48. Mouser VHM, Arkesteijn ITM, van Dijk BGM, Wuertz-Kozak K, Ito K . Hypotonicity differentially affects inflammatory marker production by nucleus pulposus tissue in simulated disc degeneration versus herniation. *J Orthop Res*. 2019;37:1110-1116.
49. Li Z, Gehlen Y, Heizmann F, et al. Preclinical ex-vivo testing of anti-inflammatory drugs in a bovine intervertebral degenerative disc model. *Front Bioeng Biotechnol*. 2020;8(583):1-23.
50. Kamali A, Ziadlou R, Lang G, et al. Small molecule-based treatment approaches for intervertebral disc degeneration: current options and future directions. *Theranostics*. 2021;11(1):27-47.
51. Maroudas A. Biophysical chemistry of cartilaginous tissues with special reference to solute and fluid transport. *Biorheology*. 1975;12(3–4):233-248.
52. Travascio F, Valladares-Prieto S, Jackson AR. Effects of solute size and tissue composition on molecular and macromolecular diffusivity in human knee cartilage. *Osteoarthr Cartil Open*. 2020;2(4):100087.
53. Mao H, Chen Q, Han B, et al. The effect of injection volume on disc degeneration in a rat tail model. *Spine*. 2011;36(16):E1062-E1069.
54. Elliott DM, Yerramalli CS, Beckstein JC, Boxberger JI, Johannessen W, Vresilovic EJ. The effect of relative needle diameter in puncture and sham injection animal models of degeneration. *Spine*. 2008;33(6):588-596.
55. de Wildt B, Mouser VHM & de Vries SAH et al. Notochordal cell-derived matrix hydrogel to restore biomechanics of the degenerated intervertebral disc. In: ESBiomech Conference Vienna; 2019.
56. Crispim JF, Ito K. De novo neo-hyaline-cartilage from bovine organoids in viscoelastic hydrogels. *Acta Biomater*. 2021;128:236-249.

SUPPORTING INFORMATION

Additional supporting information may be found in the online version of the article at the publisher's website.

How to cite this article: Salzer E, Mouser VHM, Tryfonidou MA, Ito K. A bovine nucleus pulposus explant culture model. *J Orthop Res*. 2022;40:2089-2102. doi:10.1002/jor.25226